Charge Transport and Recombination in a Nanoscale Interpenetrating Network of n-Type and p-Type Semiconductors: Transient Photocurrent and Photovoltage Studies of TiO_2/Dye/CuSCN Photovoltaic Cells

Brian C. O'Regan* and Frank Lenzmann

Energy Research Center Netherlands, PO Box 1, 1755 ZG Petten, The Netherlands

Received: June 6, 2003; In Final Form: November 15, 2003

Solid-state dye-sensitized photovoltaic cells have been fabricated with TiO_2 as the electron conductor and CuSCN as the hole conductor. These cells involve the nanoscale mixing of crystalline n-type and p-type semiconductors in films that are more than 100 times thicker than the individual n- and p-type domains. Charge transport and field distribution in this kind of material are as yet unexplored. We have used photocurrent and photovoltage transients, combined with variation in the layer thickness, to examine the limiting factors in charge transport and recombination. Charge transport ($t_{1/2} \approx 200\ \mu s$) is found to be similar to that in dye-sensitized electrolyte cells. Recombination at V_{oc} ($t_{1/2} \approx 150\ \mu s$) is 10 times faster than in electrolyte cells, and recombination at short circuit ($t_{1/2} \approx 450\ \mu s$) is 100 times faster. In the solid-state cells, the similarity of the charge transport and recombination rates results in a low fill factor, and photocurrent losses, both important limiting factors of the efficiency. A simple model is given, and suggestions are made for improvements in efficiency.

Introduction

Solid-state dye-sensitized solar cells are an offshoot technology of the dye-sensitized liquid-junction cells that have been under active development for the past decade.[1−12] Solid-state dye-sensitized cells have also been referred to as dye-sensitized heterojunctions (DSHs) by virtue of the placement of the light-absorbing dye at an otherwise transparent n−p heterojunction.[13,14] The promise of DSHs in the realm of photovoltaics is the fusion of the inexpensive materials of the dye-sensitized liquid-junction technology with the easier and less expensive manufacturing and packaging applicable to solid devices.[15−18]

In dye-sensitized cells, light absorption occurs in a monolayer of dye at the interface between a transparent oxide electron conductor (usually TiO_2) and a transparent electrolyte. Sufficient light absorption is achieved by using a thick layer ($\sim 10\ \mu m$) of nanosized oxide particles (~ 20 nm), wherein all of the internal surface is coated with the dye. In the liquid electrolyte cells, the pores are completely filled with the electrolyte. A solid-state version of this cell requires the filling of the pores with a solid, transparent hole conductor. This nanocomposite has a structure that has been referred to as an "interpenetrating network heterojunction" or a "bulk heterojunction". We will use interpenetrating heterojunction or the abbreviation i-het.

One of the proposed materials for the p-type side of a DSH is CuSCN.[13,19,20] In continuing our research into the combination TiO_2/dye/CuSCN, we have recently published a synthetic approach leading to the easy fabrication of cells that reach 2% energy efficiency.[21] These cells show good currents and acceptable voltages when compared to other solid-state dye-sensitized cells[17,18] or to the related polymer/fullerene cells.[22,23] However, the fill factors are frequently $\leq 50\%$, whereas $> 60\%$ is required for viable photovoltaic technology. In this paper, we use photocurrent and photovoltage transients to explore the origin of the low fill factor. Specifically, we address the question of which carrier limits charge transport (hole or electron) and whether the low fill factor is due to a high internal series resistance, a high recombination rate, or a voltage-sensitive injection efficiency.

The fabrication and functioning of the solid-state dye-sensitized devices has been presented in the literature,[21,24] and only relevant parts will be described in detail. Inside the interpenetrating p−n heterojunction, only the dye layer absorbs visible light. After a visible photon is absorbed by the dye, the excited-state dye is quenched by electron injection into the TiO_2 conduction band. The photooxidized dye is then regenerated by the capture of an electron from the valence band of CuSCN, a process also referred to as hole injection. The two photoseparated charges then percolate separately through the two phases and, in the absence of recombination, reach the front and back contacts, respectively. Recombination consists of either (a) reduction of the oxidized dye by an electron from the TiO_2 before hole injection into the CuSCN regenerates the dye or (b) recombination of an electron from the TiO_2 with a hole in the CuSCN.

Charge transport in electrolyte-filled nanoporous oxides has been extensively studied.[5,25−33] A general consensus is that electrons move through TiO_2 by diffusion rather than drift. This is because the high conductivity of the electrolyte in the pores supports only a few millivolts of voltage drop under the relatively low current densities ($\leq 20\ mA/cm^2$) involved in "one sun" operation. It is also held that, in the standard electrolytes, electron diffusion in TiO_2 is the limiting charge-transport rate as opposed to ion diffusion in the electrolyte. Furthermore, there are a large number of trap sites in or at the surface of the TiO_2, and the concentration of trapped electrons is higher than that of conduction-band electrons. If there is a built-in field at the SnO_2/(electrolyte + TiO_2) interface, then the high ionic strength

* Corresponding author. E-mail: oregan@ecn.nl.

10.1021/jp035613n CCC: $27.50
Published on Web 03/12/2004

of the electrolyte will cause it to drop within 1 nm in the electrolyte and within the first few particles in the TiO_2 film.

In the dark, all of the traps higher in energy than the redox potential of the I_3^-/I^- electrolyte will be empty. Under illumination, injected electrons will be trapped, and the Fermi level in TiO_2 will move up accordingly. As the Fermi level moves up, the concentration of conduction-band electrons will increase until an equilibrium between injection, transport, and recombination is reached at each point. At short circuit, the equilibrium Fermi level will vary across the TiO_2 film such that there is a gradient in the conduction-band electrons sufficient to carry the current.[5] It has also been proposed that there are conditions where the trap density is sufficiently large that the photocurrent can be carried by hopping via the traps rather than by movement only via the conduction band.[34]

The slow recombination rate in the I_3^-/I^- electrolyte cells is determined largely by the chemistry of the recombination reaction. The initial step is thought to be the reduction of iodine rather than tri-iodide.[32] Because the electrolytes contain at least a 5-fold excess of iodide, iodine is present at very low concentrations, and thus recombination is slow. For solid-state dye-sensitized cells, where the hole moves by electronic rather than ionic conduction, the charge-transport and recombination rates have not yet been measured. This paper quantifies these parameters for the TiO_2/dye/CuSCN system and also determines the probable cause for the high recombination rate observed in TiO_2/CuSCN interfaces, even at low applied voltages.

The dark conductivity of doped CuSCN, though smaller than most of the electrolytes, is still several orders of magnitude larger than that of porous TiO_2 films. Thus, the dark concentration of holes in CuSCN is much larger than that of electrons in TiO_2. It is reasonable to assume that the illumination of TiO_2/CuSCN cells changes mainly the Fermi level in TiO_2, analogous to the situation in TiO_2/electrolyte cells. We additionally assert that there is no built-in field across most of the TiO_2/dye/CuSCN i-het film. We have measured the dark capacitance of the SnO_2/flat-TiO_2/gold and SnO_2/flat-TiO_2/CuSCN junctions.[35] From the lower capacitance of the second junction, we can calculate that there is an ~50-nm depletion layer in the CuSCN at this interface. The depletion layer in the TiO_2/dye/CuSCN composite may be somewhat thicker; however, we can be reasonably confident that the built-in field will occupy a small fraction of the 4-μm-thick i-het films used in this study. In the rest of the film, the charges will move by diffusion.

Methods

Transparent conductive SnO_2 glass (LOF Tec 8, nominal resistance 8 Ω/sq) was purchased from Pilkington. A thin solid film of TiO_2 (30−100 nm) was deposited on the SnO_2 by spray pyrolysis.[36] Following this, a thin layer (<100 nm) of porous TiO_2 was deposited by spin coating the samples with a solution of 3% (v/v) titanium(IV) isopropoxide in ethanol. This layer was used to improve the adherence of the following layers. Mesoporous TiO_2 layers were pressed onto the spin layer using an approach based on that of Lindström et al.[37] First, 2 g of TiO_2 powder (Degussa P25, average diameter 25 nm) was suspended in 10 mL of pure ethanol by stirring for several hours, followed by 5 min of sonication using a titanium horn immersed in the suspension. The sonication duty cycle was 25% or less to avoid overheating and evaporation of the ethanol. The slurry was spread onto the surface of the SnO_2/TiO_2 substrate by tape casting (doctor blading) using one or more layers of adhesive tape (50 μm) as spacers. The resulting layer of ethanol/TiO_2 was allowed to dry in the ambient atmosphere. The very loose film of particles that results was then pressed at 500 kg/cm^2 for 60 s. The material contacting the TiO_2 during pressing was household aluminum foil. Further details on the pressed P25 layers can be found in the literature.[21,37] To make TiO_2 films <1 μm thick, the slurry was diluted and applied by spin coating. All TiO_2 layers were heated for 1−2 h at 450 °C in air prior to dyeing. Films were removed from the oven at ~100 °C and placed in ethanolic solutions of dye "N3", which is $RuL_2(SCN)_2$ where L = 4,4′-dicarboxy-2,2′-bipyridine. The dye was purchased from Solaronix under the name Ruthenium 535. In this form, the dye is intended to have four protons as counterions. After dyeing overnight, the films were rinsed in ethanol and dried by pressing the TiO_2 side down on absorbent paper. Directly after drying, the samples were placed onto the 80 °C hotplate used for CuSCN deposition.

To make the CuSCN deposition solution, 0.2 g of CuSCN was dissolved in 10 mL of *n*-propylsulfide, $(CH_3CH_2CH_2)_2S$.[19] CuSCN was purchased from Aldrich and used as received. Propylsulfide was purchased from Aldrich and Merck and checked for purity using GC−MS. All samples exceeded the rated purity (~98%), but some batches were significantly more pure. Batches with lower concentrations of the impurities propanethiol and dipropyl disulfide were selected for use. This choice was made to avoid the reactions of thiols with copper ions[38] and the higher boiling point of the disulfide. Other typical impurities, such as isomers, were judged not likely to be harmful.

Because CuSCN dissolves slowly in propylsulfide, the mixture was stirred overnight and then allowed to settle for at least 1 additional day. The amount added is slightly greater than the amount soluble and thus leaves a powder on the bottom of the vessel. Over a few days, this powder recrystallizes into rosettes of needles. After the conversion of the powder into needles, the solutions take on a slightly yellow color and, on average, give better results than freshly mixed solutions. The reason for this is unknown. Solutions were doped with Cu(II) $(SCN)_2$, which was prepared by precipitation from a water solution of LiSCN and $Cu(ClO_4)_2$. The mole ratio of Cu(II) to Cu(I) was 2%; however, it is clear that the final mole ratio in the film is considerably lower than this because of the loss of Cu(II) via the oxidation of thiocyanate. For deposition, aliquots of 2 mL were removed from the supernatant and diluted with 150 μL of propylsulfide before being used. The final solution contains approximately 0.5% (v/v) CuSCN.

The deposition of CuSCN into the pores of TiO_2 was carried out using a custom-built apparatus designed for making multiple thin layers of low-solubility materials. The apparatus consists of a movable hot stage onto which the sample is placed. The solution is dispensed onto the surface of the moving sample from a horizontal stainless steel needle (0.7 mm), closed at the end and having a line of small (~0.3 mm) holes along the top (Figure 1). The solution is pumped through the needle at 10−20 μL/min using a standard syringe pump. (Note that all plastic surfaces that come in contact with propylsulfide should be checked for compatibility; several standard plastic tubings were found to swell or dissolve.) The needle was placed ~0.5 mm from the surface, close enough that a bead of solution (~10 μL) filled the space between the needle and the surface. The sample was driven back and forth under the needle at 1.5 mm/s, a rate sufficiently slow that each part of the surface of a 1.7-cm-long sample was dry before the bead of solution passed over again. In this way, multiple thin films could be built up automatically, with a drying step between each layer. To fill a 4-μm porous TiO_2 film, ~60 coating steps were used. In addition to the material in the pores, this creates a film of ~1 μm of

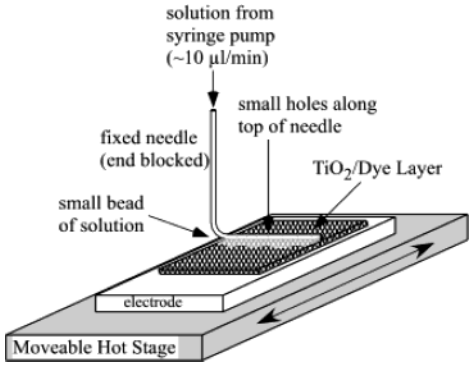

Figure 1. Diagram of the deposition method for CuSCN. For details, see the text.

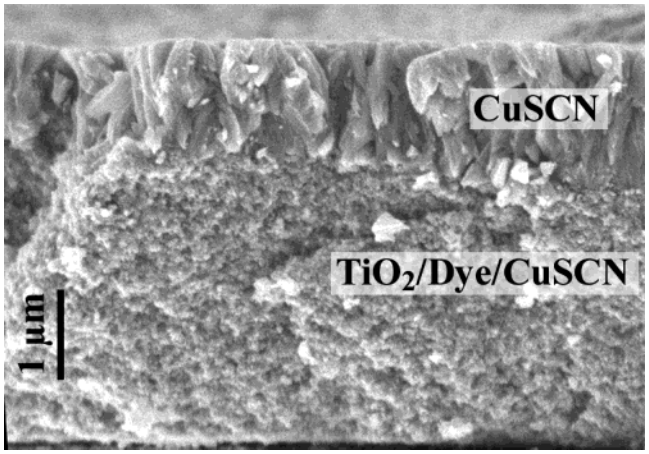

Figure 2. Cross-section SEM of the TiO_2 layer with CuSCN.

pure CuSCN on top of the porous TiO_2 layer (Figure 2). The resulting composite cells were treated under "low" vacuum ($\sim 5 \times 10^{-2}$ mbar) for 2 h and then stored under nitrogen for several days before measurement. An improvement in performance was noted during storage in nitrogen, presumably because of the continued slow outgassing of the solvent from the CuSCN layer.[21]

Photocurrent versus voltage measurements were taken using illumination from a Steuernagel solar simulator. Photocurrent and photovoltage transients were taken using a flash lamp, a potentiostat (Autolab), and bias light from two 10-W Solarc lamps (WelchAllyn). The flash was strongly attenuated by neutral density filters so that the peak intensity was about ~0.3 sun. The intensity was further modified to keep the peak voltage in voltage transients ≤ 20 mV. For current transients, the peak current of the transient was kept at $\leq 10\%$ of the steady-state current. Increasing the peak intensity of the flash by a factor of 5 did not change the time constants of the transients measured except for in the voltage transients measured in near-dark conditions, where the brighter flash caused a faster response. The length of the flash was ~100 μs, the decay half time at the end of the flash is 20 μs, and the time resolution of the potentiostat is 20 μs; thus we could measure transient phenomena with time constants ≥ 40 μs. Both the flash and bias light were "white" and incident on the front (SnO_2) side of the cell in an effort to make the measurements under real operating conditions. It is important to note that both the Steuernagel and Solarc light sources contain a UV component similar to that found in sunlight. The TiO_2/N3/CuSCN cells usually show much better performance under such illumination than under incandescent lamps lacking UV.[24]

In both the photocurrent and photovoltage transients, the decays are close to single-exponential. However, a double-exponential fit usually reduces χ^2 by a factor of 5. The two exponential time constants typically differ by less than a factor of 4, and the faster decay accounts for 70−90% of the full decay. To avoid undue complexity in the presentation, we will report and discuss only the time for the transient to decay to half of the peak value ($t_{1/2}$).

In these cells, where recombination losses at $V = 0$ are not negligible (as will be seen below), the photocurrent decays do not directly measure charge transport but only the total rate of decay of the electrons by recombination and escape to the external circuit. Moreover, even in the absence of recombination, the photocurrent decay is not really a good transport measurement. This is because electrons created by photons absorbed at different distances from the SnO_2/TiO_2 contact will require different times to diffuse to this contact. The photocurrent decay is a sum of the transport over different lengths and thus may also depend on the spectral distribution of the bias and flash illumination. In light of this, we will use the term charge-extraction half time ($t_{1/2}^{Ce}$) for the numerical results of the photocurrent transients and the term charge transport when speaking in a general sense.

It is possible to convert the photocurrent decay times, measured in the presence of recombination, into charge extraction times that would hold without recombination. One method is to assume that all absorbed photons result in injected electrons. Then, the fraction of electrons that are lost to recombination (L) is the ratio of the measured photocurrent (J_m) to the electron injection flux (J_{inj}). Knowing L, we can calculate the recombination half time by $t_{1/2}^{Rec} = t_{1/2}^{J}/L$, and the charge-extraction half time is $t_{1/2}^{Ce} = 1/(1/t_{1/2}^{J} - 1/t_{1/2}^{Rec})$, where $t_{1/2}^{J}$ is the half time of the photocurrent decay. The injection flux can be set to the photocurrent of identical TiO_2/dye films in lithium iodide electrolytes, where the internal quantum efficiency is known to be near 1. Alternately, the injection flux can be calculated from the plateau photocurrent of the TiO_2/dye/CuSCN cells at low light levels where photocurrent losses are smaller. These methods give similar results for most TiO_2/dye/CuSCN cells with TiO_2 films of ≤ 4 μm.

The above calculations of recombination and charge-extraction times at $V = 0$ assume that charge-separation efficiencies are similar in electrolyte cells and CuSCN cells or that the charge-separation efficiency is not a function of the light level in TiO_2/dye/CuSCN cells. To test these assumptions, we have attempted to measure the recombination rate when the cell is at short circuit under 1 sun illumination. This was accomplished by measuring photovoltage transients, under bias illumination, with the cell under galvanostatic control. When a constant current is set equal to the short-circuit photocurrent, a potential near $V = 0$ is maintained at the SnO_2 contact. When a light pulse is applied, the galvanostat must increase the voltage to counter the increase in current that would be caused by the increase in the photoinjected electron concentration in the porous TiO_2 film. Because the current and bias light are constant, the excess electrons can leave the TiO_2 only by recombination. The decay of the measured voltage thus measures the recombination rate at the applied voltage. We should point out, however, that if the Fermi level profile across the i-het film is steep then the recombination rate will also vary across the film and the galvanostatic experiment will measure an average recombination rate, not necessarily correctly weighted by the concentration of electrons in each part of the film.

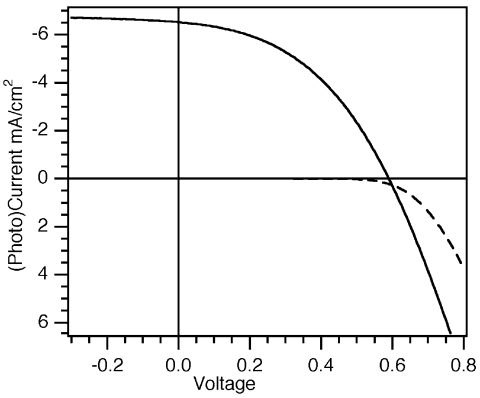

Figure 3. Dark- and photocurrent vs voltage for a typical TiO_2/N3/CuSCN cell. Illumination was ~100 mW/cm^2, simulated AM1.5.

As described below, for most TiO_2/dye/CuSCN cells, the galvanostatic voltage transients give recombination rates that agree well with the recombination rates calculated from photocurrent losses and photocurrent transients (±20% or better). This agreement is evidence that the galvanostatic experiment does measure a reasonable average recombination rate across the i-het film. The agreement also allows us to be confident in the calculation of the charge-extraction time and the comparison of electron transport in TiO_2/dye/electrolyte and TiO_2/dye/CuSCN cells. Although not the subject of this paper, we note that the two recombination-rate measurements diverge for cells degraded by heat, light, or solvent exposure.

Results and Discussion

Figure 3 shows a typical current/voltage (*I*/*V*) curve for a TiO_2/N3/CuSCN cell made with pressed and sintered P25. For this cell, the short-circuit photocurrent was 6.5 mA/cm^2, the V_{oc} was 590 mV, the fill factor was 44%, and the energy efficiency was 1.7%. Although we have made better cells, the *I*/*V*s in Figure 3 are typical of TiO_2/N3/CuSCN cells made without special treatments. As can be seen, an important limit of the efficiency of this cell is the low fill factor. For comparison, good TiO_2/N3/electrolyte cells have fill factors of 70%.[3] The photocurrent is also insufficient. This is in part due to the lack of complete light absorption, which is due to the relatively thin (4 μm) TiO_2 film used. There is, however, some reduction of the photocurrent relative to that of the same 4-μm film placed in an electrolyte cell. This can be caused by either decreased charge-separation efficiency or recombination losses at $V = 0$. Decreased charge injection could come about by incomplete pore filling or quenching of the excited state by means other than electron injection into TiO_2.

Figure 4a compares photocurrent transients from a cell containing a flat TiO_2/N3/CuSCN interface with transients from cells containing interpenetrating heterojunctions (i-hets) of 0.5 and 4 μm. The transients were measured under a continuous bias illumination of ~80 mW/cm^2. All of the photocurrent transients have been normalized to the same peak height. Figure 4a also shows the profile of the flash measured with a fast-response silicon photocell. Two different flat-interface cells were measured: SnO_2/spray-TiO_2/dye/CuSCN and SnO_2/spray-TiO_2/spin-Ti(OR)$_4$/dye/CuSCN. (See Methods section for details.) Each had a solid CuSCN layer of ~1-μm thickness, equivalent to the overlayer in the cells with i-het layers. Both flat interface cells gave similar results. The photocurrent transient for the flat TiO_2/N3/CuSCN interface is almost identical to the profile of the flash, whereas the transient decays of the cells with i-het films are slower and depend on the thickness of the film (Table

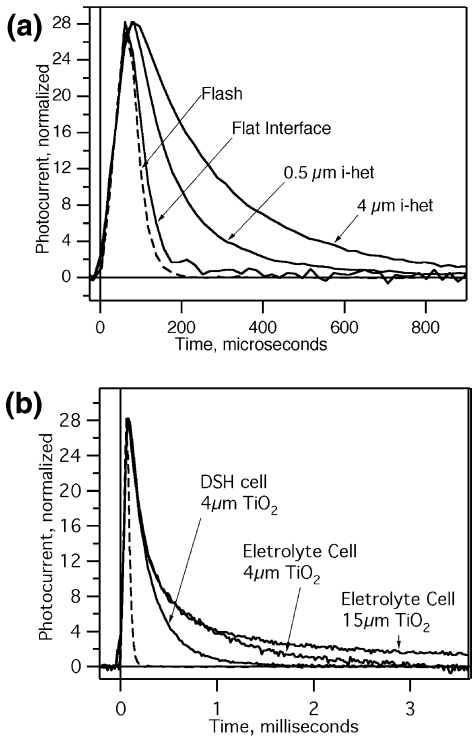

Figure 4. (a) Transient short-circuit photocurrent for a flat TiO_2/N3/CuSCN interface compared to that from two TiO_2/N3/CuSCN interpenetrating heterojunction films of 0.5 and 4 μm. Bias illumination: white light, 80 mW/cm^2. (b) Comparison of transient photocurrents for a 4-μm TiO_2/N3/CuSCN interpenetrating heterojunction, and two TiO_2/N3/electrolyte cells. The electrolyte was acetonitrile with 0.4 M hexylmethylimdazolium iodide, 50 mM I_2, 0.1 M LiI, and 0.5 M *tert*-butylpyridine. Conditions are the same as in part a.

TABLE 1: Recombination and Charge-Extraction Half Times[a] for Dye-Sensitized i-het and Electrolyte Photovoltaic Cells[b]

cell	J_{sc}[c] mA/cm^2	$t_{1/2}^{J}$ ($V = 0$)	$t_{1/2}^{Rec}$ (V_{oc})	$t_{1/2}^{Rec}$ ($V = 0$) meas[d]	$t_{1/2}^{Rec}$ ($V = 0$) calcd[e]	$t_{1/2}^{Ce}$ "meas"[f]	$t_{1/2}^{Ce}$ calcd[g]
flat DSH	0.1	≤30	620	10 ms		≤30	
0.5-μm i-het	0.75	80	200	5 ms		80	
4-μm i-het							
a	5.5	150	150	480	471	210	210
b	5.5	130	150	470	420	180	190
c	5	130	190	380	355	204	210
d	4.8	110	130	430	275	140	170
4-um EL	8	190	4 ms	100 ms		190	190

[a] In microseconds except as noted. [b] Symbols: J_{sc} = short-circuit photocurrent. $t_{1/2}^{J}$ = photocurrent decay half time. $t_{1/2}^{Rec}$ = recombination half time. $t_{1/2}^{Ce}$ = charge-extraction half time. EL = TiO_2/dye/electrolyte cell. [c] Bias light ≈ 80−100 mW/cm^2 white light. [d] Measured by galvanostatic photovoltage decay. [e] Calculated using 8 mA/cm^2 for J_{inj} (see text). [f] Calculated from columns 3 and 5. [g] Calculated from columns 3 and 6.

1) The faster decay for the flat interface shows that the slower decay from the i-het films is not limited by the RC discharge time of the underlying SnO_2/spray-TiO_2/CuSCN interface but rather by the transport of electrons and holes inside the i-het film. Additional experiments varying the cell active area and adding additional series resistance show that the measured transients are not RC-limited by the capacitance of the i-het film and the series resistance of the other components.

Figure 4b compares the photocurrent transient for a dye-sensitized i-het with those of two dye-sensitized electrolyte cells made with 4- and 12-μm TiO_2 layers, respectively. It can be seen that the early decay of all cells is similar but that the

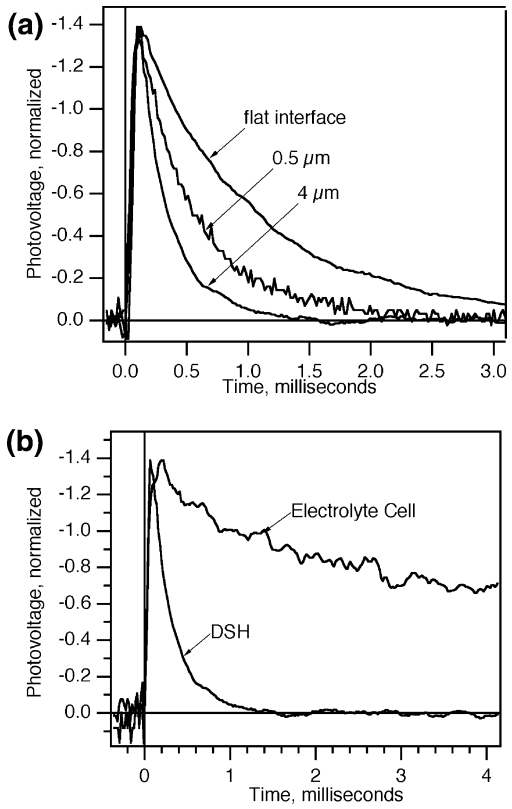

Figure 5. (a) Transient open-circuit photovoltages for a flat TiO_2/N3/CuSCN interface compared to that of TiO_2/N3/CuSCN interpenetrating heterojunctions of 0.5 and 4 μm. Bias illumination: white light, 80 mW/cm^2. (b) Comparison of transient open-circuit photovoltages for a 4-μm TiO_2/N3/CuSCN interpenetrating heterojunction and a TiO_2/N3/electrolyte cell. Bias light: 80 mW/cm^2; the electrolyte is the same as that in Figure 4b.

electrolyte cells show a longer decay at later times that itself increases with increasing TiO_2 film thickness. The photocurrent transient from the i-het cell is shortened by the recombination that occurs at $V = 0$ in these cells. To compare the transport in the two types of cells correctly, the charge extraction half time ($t_{1/2}^{Ce}$) has been calculated from the photocurrent half time ($t_{1/2}^{J}$), and the recombination losses, as detailed in the Methods section. Table 1, column 8, gives $t_{1/2}^{Ce}$ for four representative i-het films and the analogous electrolyte cell. $t_{1/2}^{Ce}$ is quite similar for all cells. Charge-extraction half times have also been calculated from the measured recombination half times ($t_{1/2}^{Rec}$) at $V = 0$. (See the Methods section and the results below.) This approach gives similar results (Table 1, column 7). We have also measured the photocurrent transients as a function of applied voltage. These measurements show that the charge-extraction time is only weakly effected by the potential; between short circuit and V_{oc}, the charge-extraction time increases by about a factor of 2 (data not shown).

As mentioned above, the photocurrent transients of standard TiO_2/dye/electrolyte cells are determined by the electron-transport characteristics of the TiO_2 films rather than by ion transport in the solution. The similar charge-extraction times for i-het and electrolyte cells imply that current transport in i-het is also limited by electron transport in TiO_2, not by hole transport in CuSCN.

Figure 5a shows photovoltage transients measured at $V_{oc} =$ 580 mV using an ~80 mW/cm^2 bias light. The light intensity was changed slightly for each cell to maintain the same V_{oc}. The figure compares the same flat-interface and i-het cells used in Figure 4a. All voltage transients have been normalized to the same peak height. The actual voltage peaks were all $\leq$6 mV. The cells with i-het films show much faster voltage decays than does the cell with the flat heterojunction (Table 1). Because the addition of the i-het film accelerates the decay of the electrons, it is safe to assume that the major recombination route in the i-het cells under these conditions, (V_{oc}, ~1 sun), is via the TiO_2-particle/CuSCN interface. The alternative—recombination by transport to SnO_2 and then back across the flat TiO_2 underlayer to CuSCN—would give a voltage transient at least as slow as that shown by the flat-interface cell. Therefore, the photovoltage decay half time is a good measure of the recombination rate in the i-het film at V_{oc}.

In absolute magnitude, the voltage peak (for the same flash intensity) of the i-het cell starts higher and reaches zero faster than that of the flat-interface cell. The higher peak means that Fermi level offset caused by the pulse is larger in the TiO_2 particles than it is in the SnO_2 + solid TiO_2 substrate. Thus, just after the pulse, the Fermi level is not flat, and some electrons will move from the TiO_2 particles to the SnO_2. Because the recombination rate from the particle film is higher than that from the SnO_2, the Fermi level in the particles will fall faster, and at some point electrons will move the other way. The fact that the voltage decay in the i-het films reaches zero long before that of the flat interface indicates that even the electrons that reach the SnO_2 will recombine by first returning to the TiO_2 nanoparticles. If these electrons could only recombine via the same channels present in the flat SnO_2/TiO_2/CuSCN interface, then the last parts of the voltage decay from the i-het cell should resemble that of the flat-interface cell. By this reasoning, in the i-het cell, recombination from SnO_2 to CuSCN via tunneling or by leaking through pinholes in the flat TiO_2 film is not an important loss route at V_{oc}.

Figure 5b compares the voltage transient decays of a dye-sensitized i-het and electrolyte cell at $V_{oc} = 580$ mV. It is clear that the recombination for the i-het (150 μs) is more than an order of magnitude faster than that of the electrolyte cell (4 ms). This higher recombination rate can be ascribed in part to the difference in the electron-transfer events that make up recombination in the two cells. In the i-het cell, recombination is a one-electron reduction of a hole at the top of the CuSCN valence band or possibly trapped at the TiO_2/CuSCN interface. The top of the CuSCN valence band is likely to have a significant contribution from Cu d orbitals.[39] Copper oxidation/reduction is frequently a fast process. The concentration of free and trapped holes in CuSCN could also be higher than that of iodine in the electrolyte, where most of the iodine is bound up in tri-iodide.

The similarity of the recombination time at V_{oc} to the charge-extraction time (Table 1) can explain the low fill factor of the DSH cells. (As mentioned above, charge extraction near V_{oc} is not faster than at $V = 0$.) A high fill factor requires that the fraction of injected electrons that recombine decrease steeply as the voltage moves back from V_{oc}. This will occur if the number of electrons involved in recombination decreases or if the rate decreases or both. When the rate constants for charge extraction and recombination are equal, charge extraction cannot decrease the concentration of electrons sufficiently such that the recombination current ($J_{rec} = Q_{rec}/t_{1/2}^{Rec}$) becomes insignificant. This simplified explanation assumes that the pool of electrons that participate in recombination and transport are the same, for example, electrons in traps near the Fermi level, moving and recombining via the conduction band. Recombination and transport via traps is also a possibility; however, further elaboration of the discussion would not change the basic picture.

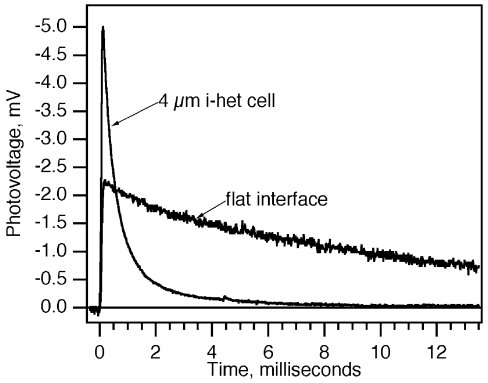

Figure 6. Transient short-circuit galvanostatic photovoltage for a flat TiO_2/N3/CuSCN interface compared to that from a TiO_2/N3/CuSCN interpenetrating heterojunction film of 4 μm. Bias illumination: white light, 80 mW/cm^2.

From the data, we can be confident that the low fill factor in the DSH cells is due to the recombination of injected charges, not to an injection efficiency that decreases with potential or to a high series resistance in the spray-TiO_2 or CuSCN layers.

As well as the poor fill factor, the DSH cells show lower short-circuit photocurrents than electrolyte cells with the same TiO_2 films. This could be due to various problems that would inhibit hole or electron injection, such as incomplete pore filling or dye desorption into the CuSCN deposition solution. Alternatively, the lower photocurrent may be due to recombination losses occurring at short circuit. To determine if the latter are occurring, we have measured the recombination rate at $V = 0$ using voltage transients under galvanostatic control. Details of the measurement are given in the Methods section.

Figure 6a shows the resulting voltage transient for the flat-interface cell compared to that from a 4-μm i-het film using the same bias light and pulse intensity. For the flat-interface cell, the time constant of the voltage decay is now 7 ms, a factor of 10 slower than that at V_{oc}. For the 4-μm i-het film, the time constant of the voltage decay at short circuit is 400 μs, only a factor of $\sim$2 slower than at V_{oc} (150 μs). Thus, near $V = 0$, the presence of the i-het film accelerates the recombination even more strongly than at V_{oc}. In addition, the transient voltage peak is higher for the i-het film. These observations show that the voltage decay measured galvanostatically is a measure of the recombination rate of electrons in the i-het film as opposed to only those electrons in the SnO_2. Thus, for the 4-μm i-het films, the recombination at $V = 0$ ($t_{1/2} \approx 450$ μs) is fast enough, relative to transport ($t_{1/2} \approx 200$ μs), to cause recombination losses. This does not preclude additional losses from incomplete pore filling and so forth; however, it does mean that attempts to use thicker films to achieve higher photocurrents can succeed only if the recombination rate at $V = 0$ can be decreased or transport can be increased.

The relatively small change in recombination rate in the i-het film between V_{oc} and $V = 0$ suggests that the change in applied bias at the SnO_2 causes only a small change in the electron concentration in the i-het film. With the SnO_2 held at $V = 0$ and photocurrent flowing, there is a gradient in the electron concentration in the TiO_2, and therefore in the Fermi level, between the dark value adjacent to the SnO_2 and some higher level in the TiO_2 at the other edge of the i-het film. An estimate of the Fermi level in the outer parts of the TiO_2 can be made as follows. At V_{oc}, because there is no current flowing, the Fermi level throughout the i-het film is equal to that measured at the SnO_2. Thus, voltage transients at V_{oc} give the recombination $t_{1/2}$ for a known Fermi level. Because the recombination $t_{1/2}$ in these cells changes rapidly with the Fermi level (see below) when there is a gradient in the Fermi level, most recombination will be occurring where the Fermi level is closest to the conduction band. Therefore, the galvanostatic voltage transient at $V = 0$, under 1 sun, is weighted heavily by the recombination in the outer part of the film. It is possible to find a light level of <1 sun such that the recombination $t_{1/2}$ at V_{oc}, at this light level, is equal to the recombination $t_{1/2}$ at $V = 0$ and 1 sun. This V_{oc} is an estimate of the Fermi level in the outer part of the TiO_2 film at short circuit. Similarly, the Fermi level in the outer part of the TiO_2 film can be estimated for other short-circuit conditions.

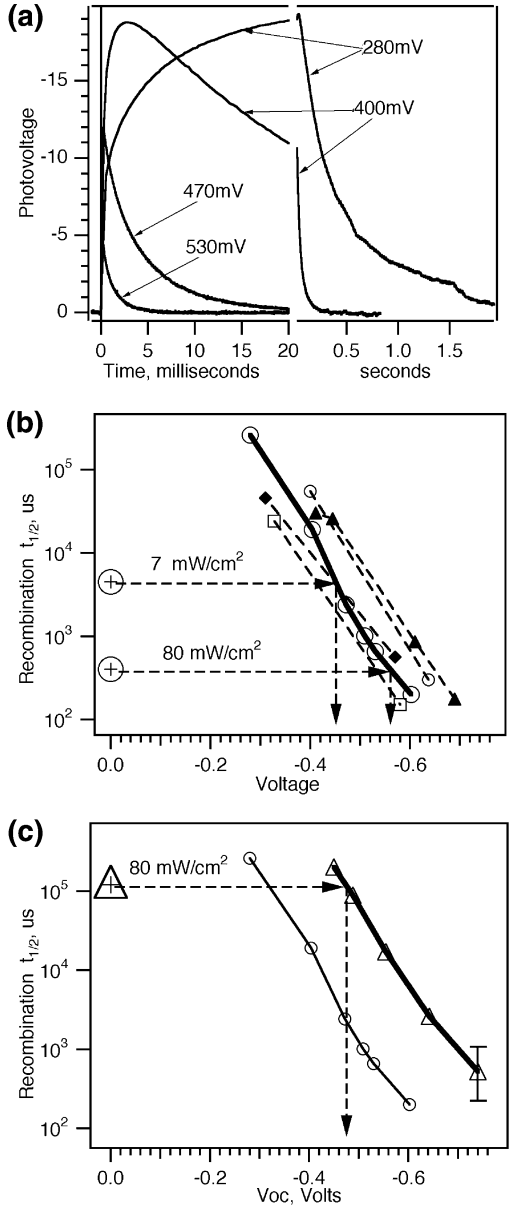

Figure 7. (a) Transient open-circuit photovoltages for a 4-μm TiO_2/N3/CuSCN i-het under different light intensities from $\sim$2.5 μW/cm^2 to 10 mW/cm^2. Labels indicate the V_{oc} at which each transient was measured. (b) Open-circuit photovoltage decay $t_{1/2}$ vs V_{oc} for five different TiO_2/N3/CuSCN i-het cells; the bold line indicates data for the 4-μm cell used in previous figures. The short-circuit galvanostatic photovoltage decay $t_{1/2}$ values for the 4-μm cell under two light levels are plotted at $V = 0$. (c) Comparison of open-circuit photovoltage decay $t_{1/2}$ vs V_{oc} for a TiO_2/N3/CuSCN cell and an electrolyte cell. Galvanostatic photovoltage decay $t_{1/2}$ for the electrolyte cell at $V = 0$.

Figure 7a presents photovoltage transients, measured at V_{oc}, for which the light intensity was varied from $\sim$2.5 μW/cm^2 to

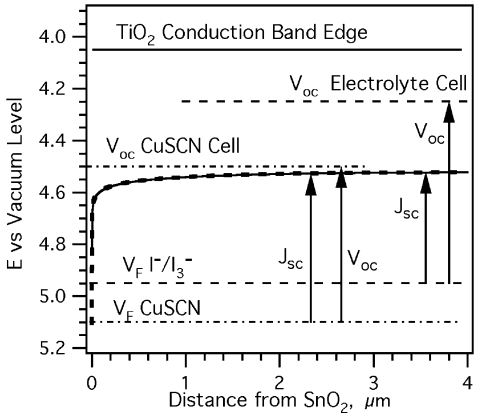

Figure 8. Comparison of Fermi levels across a 4-μm TiO_2 particle film in a TiO_2/dye/CuSCN cell and an electrolyte cell. Fermi levels shown in the dark, at V_{oc}, and carrying 1 sun of photocurrent. For the calculation of levels, see the text. The choices for V_{dark} give $n_{cb}(0)$ of $2 \times 10^5/cm^3$ and $500/cm^3$ for the iodine/iodide and CuSCN cells.

10 mW/cm^2. The rise time of the voltage becomes slower with lower bias light because of the slower electron transport at low bias light. This is because the measured voltage is that established at the SnO_2/dense-TiO_2/CuSCN interface. This interface has some capacitance, thus slower transport results in a slower build up of the measured voltage. Because the voltage decays are ~100 times slower than the rise times, the slow rise times do not affect the decay time measurement.

In Figure 7b, we have plotted the log of the voltage decay $t_{1/2}$ versus the V_{oc} for five different TiO_2/N3/CuSCN i-het cells made under various conditions. As can be seen, the slope of all of the cells is quite similar, although the rate for a given V_{oc} varies.[40] The bold line goes through the data points for the cell used for Figure 6. When the light intensity is reduced to ~2.5 μW/cm^2, the V_{oc} is 280 mV, and the voltage decay $t_{1/2}$ is 200 ms. Also plotted in Figure 7b are the voltage $t_{1/2}$ values measured galvanostatically for this cell at two different illumination levels. The points are marked by larger symbols to indicate the somewhat larger uncertainty in these values.[41] Shown graphically in Figure 7b is the V_{oc} where the recombination $t_{1/2}$ is the same as that at short circuit under bias light. The analysis indicates that in the i-het film, under 1 sun bias light, the application of $V = 0$ to the SnO_2 lowers the Fermi level in the TiO_2 to 560 mV, which is only 40 mV lower than the V_{oc} of this cell, 600 mV. When the illumination intensity is reduced by a factor of 10, the Fermi level in the TiO_2 drops to ~150 mV below V_{oc}.

To compare this to the electrolyte cell, in Figure 7c we have plotted the voltage decay $t_{1/2}$ values for an electrolyte cell versus V_{oc}. The recombination rates for a given V_{oc} are all 10 times slower than for the DSH, but the slope is similar. We have also measured the galvanostatic voltage transients for the dye-sensitized electrolyte cell. The voltage decay $t_{1/2}$ at $V = 0$ was ~100 ms. For the electrolyte cells, recombination at $V = 0$ is 500 times slower than charge extraction, and little recombination loss will occur, as is already known from the near-100% internal quantum efficiency. Comparing the recombination at V_{oc} and $V = 0$, we see that, for the electrolyte cell, the application of $V = 0$ to the SnO_2 lowers the Fermi level in the TiO_2 by 240 mV relative to V_{oc}.

The difference between the electrolyte and solid-state cells can be understood by reference to Figure 8. Figure 8 shows the various energy levels in both cells on the vacuum scale. Before discussing Figure 8, we caution against placing undue emphasis on the absolute values displayed. Because of uncertainties in relating NHE to the vacuum scale, uncertainty in the diffusion constant of electrons in the TiO_2, and changes in the TiO_2 conduction-band energy with different adsorbates, we intend this figure to be only semiquantitative.

To construct Figure 8, we have used the following values. The potential of the I^-/I_3^- redox couple in the organic electrolyte is ~0.3 V versus NHE, thus 4.95 versus vacuum. We have used 4.65 for the potential of NHE on the vacuum scale, chosen as the center of a range of published estimates, 4.5 to 4.8. We have measured the work function, in the dark, of doped CuSCN to be ~5.1 V. To find the Fermi level in the TiO_2 at V_{oc}, we add the measured V_{oc} for each cell to the dark potential of their respective hole conductor.

In Figure 8, we have also plotted the calculated Fermi level profile through a 4-μm TiO_2 film when carrying a short-circuit photocurrent of 6 mA/cm^2 (~1 sun). The profile was calculated following the method of van de Lagemaat et al. (eqs 1 and 2).[5] Briefly, by knowing the incident light intensity (I_o) and the optical density (α), one can calculate the photocurrent at each distance from the SnO_2. Then, using a diffusion constant for conduction-band electrons (D_{cb}), one calculates the concentration profile of conduction-band electrons (n_{cb}) required to carry the photocurrent. The concentration of conduction-band electrons fixes the depth of the Fermi level (V_F) below the conduction-band energy (V_{cb}).

$$n_{cb}(x) = n_{cb}(0) + \frac{I_o}{D_{cb}}\left[\frac{1}{\alpha} - x e^{-\alpha L} - e^{-\alpha x}\right] \qquad (1)$$

where x is the distance from the SnO_2/TiO_2 contact, L is the

$$[V_F - V_{cb}](x) = kT^* \ln\left(\frac{n_{cb}(x)}{N}\right) \qquad (2)$$

thickness of the TiO_2 film (4 μm), $n_{cb}(0)$ is the electron concentration in the TiO_2 next to the SnO_2, and N is the density of states at the TiO_2 conduction-band edge ($1021/cm^3$).[5] We use $D_{cb} = 1$ cm^2/s[42] for both the electrolyte and i-het cells. Note that as long as the TiO_2 films are identical and electron transport is limiting, the Fermi-level profile in the TiO_2 does not depend on the hole-conducting medium, except in the last few nanometers adjacent to the SnO_2. Adjacent to the SnO_2, at $V = 0$, the Fermi level in the TiO_2 is set by the Fermi level in the hole conductor. However, the steep gradient in electron concentration away from the SnO_2 results in effectively equal concentrations away from the SnO_2 and thus equal Fermi levels. In calculating the values shown in Figure 8, we have used a weighted-average optical density that reproduces the observed photocurrent. This will give a single-exponential decay of the white light, which is not exact.

In Figure 8, we have arbitrarily chosen a potential of 4.05 V versus vacuum for the conduction-band edge of TiO_2 in both cells. This value places the calculated Fermi-level profile in the TiO_2 ~40 mV below the Fermi level at V_{oc} for the TiO_2/dye/CuSCN cell. This makes Figure 8 consistent with the measurements shown in Figure 7b. This choice then fixes the difference between the two Fermi levels for the electrolyte cell at ~290 mV. Considering that we have not adjusted any parameters, this is acceptably close to the 240 mV found from Figure 7c. Simply replacing 4.65 with 4.7 V for the vacuum potential of NHE would make the agreement quantitative.

Also, 4.05 V is not unreasonable for the conduction-band edge of TiO_2. From flatband measurements in aqueous solution, a conduction-band edge potential of 4.05 V would occur at a pH ~8.[43,44] Because the CuSCN deposition solution contains

no acidic protons and SCN^- is known to adsorb to TiO_2, a negative surface charge corresponding to pH 8 is reasonable. We note that the electrolyte cell that was tested had *tert*-butylpyridine (TBP) in the electrolyte, which is known to increase the voltage, in part by causing an upward shift in the TiO_2 conduction band.[17,45] An upward shift of the conduction band in the electrolyte cell, relative to the CuSCN cell, would also make Figures 7c and 8 more consistent.

Figure 8 illuminates the difference between the electrolyte and CuSCN cells. In the CuSCN cell, 1 sun illumination at open circuit moves the V_F in the TiO_2 negative of the dark level; however, the high recombination rate limits V_F to ~400 mV below the conduction band. Because of the transport characteristics of the TiO_2, under 1 sun, the application of bias voltage to the SnO_2 can only reduce the V_F to ~450 mV below the conduction band. This does not sufficiently reduce the recombination rate, which causes low fill factors and recombination losses at short circuit. In the electrolyte cell, the intrinsically lower recombination rate constant allows the Fermi level at V_{oc} to move up to 200 mV below the conduction band. The application of bias to the SnO_2 electrode can thus reduce the V_F by ~250 mV, leading to a large reduction in the recombination rate and efficient charge collection.

Thus, the model reproduces the observed behavior in Figure 7b and c. Note that the model predicts that a small increase or decrease in D_{cb}, due, for example, to a different source of TiO_2 particles, should have a larger impact on the fill factor of the solid state-cells than the liquid-electrolyte cells. In fact, we do find that the exact TiO_2 that is used is more critical for the CuSCN cells than the electrolyte cells.

Figure 8 can also be used to explain another interesting feature of the TiO_2/dye/CuSCN cells. From both the transient peak heights and impedance measurements, we find that the capacitance of the DSH cells is $\leq 50\ \mu F/cm^2$ at V_{oc}. This is very different from the ~1 mF/cm^2 measured for the electrolyte cells at V_{oc}. The capacitance in both cells is controlled by the trap-state density near the Fermi level in the TiO_2 particles. Figure 8 shows that in the DSH cells at V_{oc} the Fermi level is close to that in the electrolyte cells ~200 mV below V_{oc}. In agreement, the capacitance of equivalent electrolyte cells, 200 mV below V_{oc}, is about 50 $\mu F/cm^2$.

We note in passing that the measured dependence of the recombination on the V_{oc} (Figure 7b and c) has additional implications. There can be little doubt that recombination between the electron in TiO_2 and the hole in the CuSCN is a one-electron reaction. Therefore, if we were to assume that all of the electrons in the TiO_2 are equal, then the reaction should be first order, and the rate constant should not depend on the electron concentration and thus not on the voltage. Obviously, from Figure 7, this is not the case because the rate constant does depend on the voltage. A similar dependency of recombination rate on potential has been observed for solid-state dye-sensitized cells using a molecular hole conductor, which should also involve a one-electron reduction.[46] One current explanation for the dependence of the recombination rate on voltage in the iodide electrolyte cells is a second-order reaction rate implied by the recombination with iodine instead of tri-iodide.[32] The fact that recombination in TiO2/dye/electrolyte cells has the same voltage dependency as the TiO2/dye/CuSCN cells (Figure 7c), where a second-order reaction is highly unlikely, weighs against proposed explanations involving specifics of the iodine/iodide reaction kinetics.

Conclusions

In summary, we have shown that charge extraction in TiO_2/dye/CuSCN cells is limited by the electron-transport characteristics of the TiO_2, with an electron diffusion constant similar to that of equivalent TiO_2 electrolyte cells. We have found that the recombination rate for a given electron concentration is much faster for the TiO_2/CuSCN interface than for the TiO_2/(I_3^-/I^- electrolyte) interface. For the CuSCN cell, the similarity of the charge extraction and recombination rates at all voltages (under illumination) creates the poor fill factor and is responsible for some losses of photocurrent at short circuit. The most obvious way to improve the TiO_2/dye/CuSCN cells is to reduce the recombination rate. This can be accomplished by surface treatments, as already reported for liquid junction cells.[11,47] Another approach is to increase the electron-transport rate in the TiO_2. Although recipes to accomplish this are not yet known, the variation in transport rates between different TiO_2 sources and treatments [9] argues that it should be possible.

Acknowledgment. Funding for this work was supplied by the Dutch Ministry of Economic Affairs (ECN subsidy) and the European Commission Project HPRN-CT-2000-00-0141 (F.L.).

References and Notes

(1) Desilvestro, J.; Gratzel, M.; Kavan, L.; Moser, J.; Augustynski, J. *J. Am. Chem. Soc.* **1985**, *107*, 2988.
(2) O'Regan, B.; Grätzel, M. *Nature* **1991**, *353*, 737.
(3) Nazeeruddin, M. K.; Péchy, P.; Renouard, T.; Zakeeruddin, S. M.; Humphry-Baker, R.; Comte, P.; Liska, P.; Cevey, L.; Costa, E.; Shklover, V.; Spiccia, L.; Deacon, G. B.; Bignozzi, C. A.; Grätzel, M. *J. Am. Chem. Soc.* **2001**, *123*, 1613.
(4) Hinsch, A.; Kroon, J. M.; Kern, R.; Uhlendorf, I.; Holzbock, J.; Meyer, A.; Ferber, J. *Prog. Photovoltaics* **2001**, *9*, 425.
(5) van de Lagemaat, J.; Frank, A. J. *J. Phys. Chem. B* **2000**, *104*, 4292.
(6) Kuciauskas, D.; Freund, M. S.; Gray, H. B.; Winkler, J. R.; Lewis, N. S. *J. Phys. Chem. B* **2001**, *105*, 392.
(7) Gillaizeau-Gautheir, I.; Odobel, F.; Alebbi, M.; Argazzi, R.; Costa, E.; Bignozzi, C. A.; Qu, P.; Meyer, G. J. *Inorg. Chem.* **2001**, *40*, 6073.
(8) Gregg, B. A.; Pichot, F.; Ferrere, S.; Fields, C. L. *J. Phys. Chem. B.* **2001**, *105*, 1422.
(9) Nakade, S.; Matsuda, M.; Kambe, S.; Saito, Y.; Kitamura, T.; Sakata, T.; Wada, Y.; Mori, H.; Yanagida, S. *J. Phys. Chem. B* **2002**, *106*, 10004.
(10) Yoshida, T.; Oekermann, T.; Okabe, K.; Schlettwein, D.; Funabiki, K.; Minoura, H. *Electrochemistry* **2002**, *70*, 470.
(11) Palomares, E.; Clifford, J.; Haque, S. A.; Lutz, T.; Durrant, J. R. *J. Am. Chem. Soc.* **2003**, *125*, 475.
(12) Chappel, S.; Chen, S. G.; Zaban, A. *Langmuir* **2002**, *18*, 3336.
(13) O'Regan, B.; Schwartz, D. T. *Chem. Mater.* **1995**, *7*, 1349.
(14) O'Regan, B.; Schwartz, D. T. Efficient Photo-Hole Injection from Cyanine Dyes into CuSCN: A Prospective p-Type Material for a Dye Sensitized p−n Heterojunction. *Nanostructured Materials in Electrochemistry*; Reno, NV, 1995, The Electrochemical Society: Pennington, NJ.
(15) Krüger, J.; Plass, R.; Grätzel, M.; Matthieu, H. J. *Appl. Phys. Lett.* **2002**, *81*, 367.
(16) Perera, S.; Senadeera, R.; Tennakone, K.; Ito, S.; Kitamura, T.; Wada, Y.; Yanagida, S. *Bull. Chem. Soc. Jpn.* **2003**, *76*, 659.
(17) Krüger, J.; Plass, R.; Cevey, L.; Piccirelli, M.; Grätzel, M.; Bach, U. *Appl. Phys. Lett.* **2001**, *79*, 2085.
(18) Kumara, G. R. A.; Konno, A.; Shiratsuchi, K.; Tsukahara, J.; Tennakone, K. *Chem. Mater.* **2002**, *14*, 954.
(19) Kumara, G. R. R. A.; Konno, A.; Senadeera, G. K. R.; Jayaweera, P. V. V.; De Silva, D. B. R. A.; Tennakone, K. *Sol. Energy Mater. Sol. Cells* **2001**, *69*, 195.
(20) Tennakone, K.; Kahanda, M.; Kasige, C.; Abeysooriya, P.; Wijayanayaka, R. H.; Kaviratna, P. *J. Electrochem. Soc.* **1984**, *131*, 1574.
(21) O'Regan, B.; Lenzmann, F.; Muis, R.; Wienke, J. *Chem. Mater.* **2002**, *14*, 5023.
(22) Shaheen, S. E.; Brabec, C. J.; Sariciftci, N. S.; Padinger, F.; Fromherz, T.; Hummelen, J. C. *Appl. Phys. Lett.* **2001**, *78*, 841.
(23) Kroon, J. M.; Wienk, M. M.; Verhees, W. J. H.; Hummelen, J. C. *Thin Solid Films* **2002**, *403*, 223.

(24) O'Regan, B.; Schwartz, D. T. *Chem. Mater.* **1998**, *10*, 1501.
(25) Cao, F.; Oskam, G.; Meyer, G. J.; Searson, P. C. *J. Phys. Chem.* **1996**, *100*, 17021.
(26) Yoshida, T.; Shinada, A.; Oekermann, T.; Sugiura, T.; Sakai, T.; Minoura, H. *Electrochemistry* **2002**, *70*, 453.
(27) Nelson, J.; Eppler, A. M.; Ballard, I. M. *J. Photochem. Photobiol., A* **2002**, *148*, 25.
(28) Kambe, S.; Nakade, S.; Wada, Y.; Kitamura, T.; Yanagida, S. *J. Mater. Chem.* **2002**, *12*, 723.
(29) O'Regan, B.; Moser, J.; Anderson, M.; Gratzel, M. *J. Phys. Chem.* **1990**, *94*, 8720.
(30) Solbrand, A.; Lindstrom, H.; Rensmo, H.; Hagfeldt, A.; Lindquist, S.-E.; Sodergren, S. *J. Phys. Chem. B* **1997**, *101*, 2514.
(31) van Roosmalen, J. A. M.; O'Regan, B. C.; Kroon, J. M.; Sinke, W. C. Dye Sensitized Solar Cells. In *Handbook of Photochemistry and Photobiology*; Nalwa, H. S., Ed.; American Scientific Publishers: Stevenson Ranch, CA, 2003; Vol. 1, p 1.
(32) Peter, L. M.; Wijayantha, K. G. U. *Electrochem. Commun.* **1999**, *1999*, 576.
(33) de Jongh, P. E.; Meulenkamp, E. A.; Vanmaekelbergh, D.; Kelly, J. J. *J. Phys. Chem. B* **2000**, *104*, 7686.
(34) Gregg, B. A.; Chen, S. G.; Ferrere, S. *J. Phys. Chem. B* **2003**, *107*, 3019.
(35) O'Regan, B. Unpublished data.
(36) O'Regan, B.; Schwartz, D. T. *J. Appl. Phys.* **1996**, *80*, 4749.
(37) Lindström, H.; Magnusson, E.; Holmberg, A.; Södergren, S.; Lindquist, S. E.; Hagfeldt, A. *Sol. Energy Mater. Sol. Cells* **2002**, *73*, 91.
(38) Peña, M. J.; Alarcón, I.; López, V. *Electrochem. Acta* **1990**, *35*, 47.
(39) Matzdorf, R.; Skonieczny, J.; Westhof, J.; Engelhard, H.; Goldmann, A. *J. Phys.: Condens. Matter.* **1993**, *5*, 3827.
(40) The slope we find is identical to that found for electron recombination with the dye cation in Haque et al.[45] Unfortunately, most studies of recombination with the electrolyte have given the recombination rate as a function of incident intensity, which cannot be compared with our data without also knowing the V_{oc} as a function of intensity.
(41) The uncertainty in this value depends on the "flatness" of the IV curve as it goes through zero. For very flat IVs, a small change in the bias light intensity will require a large change in the voltage to maintain constant current. Because our bias illumination had slow fluctuations, possibly due to thermal fluctuations in the lamps, the galvanostatic transients for $V = 0$ were measured against a sloping baseline.
(42) Forro, L.; Chauvet, O.; Emin, D.; Zuppiroli, L.; Berger, H.; Levy, F. *J. Appl. Phys.* **1994**, *75*, 633.
(43) Duonghong, D.; Ramsden, J.; Grätzel, M. *J. Am. Chem. Soc.* **1982**, *104*, 2977.
(44) O'Regan, B.; Gratzel, M.; Fitzmaurice, D. *Chem. Phys. Lett.* **1991**, *183*, 89.
(45) Haque, S. A.; Tachibana, Y.; Willis, R. L.; Moser, J. E.; Grätzel, M.; Klug, D. R.; Durrant, J. R. *J. Phys. Chem. B* **2000**, *104*, 538.
(46) Krüger, J.; Plass, R.; Grätzel, M.; Cameron, P. J.; Peter, L. M. *J. Phys. Chem. B* **2003**, *107*, 7536.
(47) Kumara, G. R. R. A.; Tennakone, K.; Prera, V. P. S.; Konno, A.; Kaneko, S.; Okuya, M. *J. Phys. D.* **2001**, *34*, 868.